

Article

Influence of Sub-CMC Rhamnolipid Flushing on the Mobilization and Solubilization of Residual Dodecane in Saturated Porous Media

Xin Yang ¹ , Hua Zhong ^{2,*}, Guansheng Liu ³ , Lili Huo ³ and Zonghua Wang ¹

¹ College of Water Resource and Modern Agriculture, Nanyang Normal University, Nanyang 473061, China; yangx26@126.com (X.Y.); wangzonghua3511@163.com (Z.W.)

² Ningbo Institute of Digital Twin, Eastern Institute of Technology, Ningbo 315200, China

³ State Key Laboratory of Water Resources Engineering and Management, Wuhan University, Wuhan 430072, China; gslu0615@163.com (G.L.); ll_huo0315@163.com (L.H.)

* Correspondence: zhonghua21cn@126.com

Abstract: The potential of monorhamnolipid (monoRL) biosurfactant to enhance the removal of residual dodecane from a porous medium was investigated under monoRL concentration varying from sub-CMC to hyper-CMC conditions by one-dimension column experiments. In the immiscible displacement experiment, 76% of the total volume of dodecane is removed by flushing of 150 μM monoRL solution. The solubilization of dodecane could be enhanced by rhamnolipid even at monorhamnolipid concentrations as low as 50 $\mu\text{M}/\text{L}$. The higher solubilization concentration (500 $\mu\text{M}/\text{L}$) of monoRL solution results in higher solubilized dodecane concentration (160 $\mu\text{M}/\text{L}$) due to the larger quantity of micelle formation. Compared to solubilization, immiscible displacement, or mobilization, is far more effective in removing residual dodecane. The interfacial partitioning tracer tests (IPTT) method is applied to measure the variation in specific dodecane-water interface areas (A_{nw}). The results showed that the flushing of monoRL increased the A_{nw} from 2.04 to 3.54 cm^2/cm^3 . This investigation implies that low-concentration monorhamnolipid flushing and subsequent micelle solubilization is an economic method to remediate NAPL-contaminated fields.



Citation: Yang, X.; Zhong, H.; Liu, G.; Huo, L.; Wang, Z. Influence of Sub-CMC Rhamnolipid Flushing on the Mobilization and Solubilization of Residual Dodecane in Saturated Porous Media. *Water* **2024**, *16*, 3152. <https://doi.org/10.3390/w16213152>

Academic Editor: Constantinos V. Chrysikopoulos

Received: 10 September 2024

Revised: 21 October 2024

Accepted: 1 November 2024

Published: 4 November 2024



Copyright: © 2024 by the authors. Licensee MDPI, Basel, Switzerland. This article is an open access article distributed under the terms and conditions of the Creative Commons Attribution (CC BY) license (<https://creativecommons.org/licenses/by/4.0/>).

Keywords: surfactant; solubilization; NAPL; remediation

1. Introduction

Hydrophobic organic compounds (HOCs) are widespread contaminants frequently released in the shape of non-aqueous phase liquids (NAPLs). Generally, these pollutants are poorly soluble in water, while they often occur in concentrations exceeding regulatory values in groundwater. In addition, although contaminated areas are small initially, they may cause long-term threats to the public and environment because of pollutant dispersion by ground water flow. With regard to public health and safety, it is necessary and crucial to remediate these contaminated sites. Several technologies have been developed or modified to treat source areas, including surfactant flushing [1–3], chemical oxidation [4–6], in situ thermal treatment [7] and onsite bioremediation [8,9].

Although complete remediation of some NAPL sources is possible, it is more common that NAPLs cannot be completely recovered from contaminated aquifers [10]. The low solubility in aqueous and high interfacial tension between water and organic pollutants require the application of technologies, such as onsite bioremediation, pump, and treatment. For example, NAPLs may be retained in the form of trapped drops because of capillary forces. NAPLs trapped in a porous medium in the shape of residual saturation may occupy about 5 to 40 percent of pore volume [11]. Surfactants, as amphiphilic substances, are often used for enhancing the mobilization of residual NAPLs by reducing the interfacial tension and increasing the solubility of organic by micelle solubilization [12–16]. Numerous studies

have been conducted to measure the application of surfactants in the NAPLs remediation field [5,17–22]. For instance, Wu et al.'s investigation showed the flushing of 4% Tween 80 solution strongly influenced the distribution of PCE droplets in a two-dimensional sandbox experiment [23]. Jacome and Van Geel found the average removal of entrapped NAPL is as high as 45% under sodium dodecyl benzene sulfonate (SDBS) solution flooding in column tests [24]. Furthermore, Martel et al. reported that more than 89% of residual DNAPL was recovered under 0.8 pore volume of surfactant-alcohol solution flooding [10]. Pennell et al. studied the surfactant-enhanced solubilization of residual dodecane in soil columns by flushing with 43 g/L anionic surfactant (polyoxyethylene (20) sorbitan monooleate) solution, and the results indicated that the flushing increased the concentration of dodecane by five orders of magnitude [25]. Taylor et al. investigated the effect of 4% Tween 80 solution flushing on the recovery of tetrachloroethylene (PCE) from a porous medium. They found that the concentration of PCE in the effluent was improved as high as 6000 mg/L in both column and 2-D box experiments [18]. In addition, field-scale application of surfactant flushing has been conducted at sites contaminated with petroleum hydrocarbons and chlorinated solvents [26]. However, previous investigations are mostly conducted at very high surfactant concentrations. The application of high-concentration surfactant in practical NAPL remediation may cause concerns: (1) higher concentrations of surfactant increase costs and are not beneficial because of colloid migration and macroemulsion formation [27]; (2) lots of surfactants are introduced into an underground aquifer, which is probably causing secondary contamination.

Our recent studies showed the biosurfactant rhamnolipid exhibited excellent alkane-solubilization activity under sub-CMC concentration based upon aggregate-formation mechanism [28]. In addition, it showed that the mole solubilization ratio of rhamnolipid under sub-CMC is higher than at above CMC. Furthermore, rhamnolipid has low CMC (75.1 mg/L in PBS solution), making it a suitable substance for reducing interface tension at relatively low concentrations. At the same time, as a biosurfactant, rhamnolipid is environmentally friendly. Therefore, it may provide an alternative economic method using sub-CMC concentration enhanced displacement and solubilization of NAPLs to avoid the disadvantages of the conventional solubilization approach using surfactants under high concentrations. The prior studies, however, on the application of rhamnolipid in surfactant-enhanced aquifer remediation at the condition of flowing cells are few [29].

Understanding and predicting the behavior of NAPLs at contaminated sites is of fundamental interest in site remediation. To understand the retention and remediation of NAPL in saturated sites, two important characteristics should be paid much more attention: the saturation of NAPL (volume of NAPL per unit volume of pore space) and area of NAPL-water interface per unit volume of a porous medium [10]. It has long been recognized that the fluid–fluid interface plays an important role in contaminant and multiphase flow phenomena [30,31]. The interfacial partitioning tracer test (IPTT) method introduced by Saripalli et al. [32,33] is applied to measure the NAPL-water interfacial areas by column experiments and it has been applied successfully for a large quantity of applications [34–36]. The IPTT method makes it possible to indirectly measure the fluid–fluid interfacial area in the porous medium system [32,37]. For example, Brusseau and Taghavi measured the tetrachloroethene-water interfacial areas under a series of saturations and their results showed tetrachloroethene-water interfacial areas rising with the decrease in water saturation [38]. In previous studies, however, researchers usually focused on either the solubilization of HOCs or the mobilization of NAPL under the flushing of surfactants. The knowledge of overall variation in mobilization, solubilization, and the phase-specific interfacial area of NAPL in a system is limited.

The objective of this investigation is to give insight into the influence of monorhamnolipid (monoRL) flushing at a relatively low concentration on the mobilization and solubilization of residual dodecane by column experiments. MonoRL and dodecane are selected as the representative biosurfactant and hydrophobic organic compounds, respectively. Interfacial tensions are measured to characterize surface activity. Miscible displacement

and solubilization experiments are conducted through one-dimensional (1-D) column experiments under different monoRL concentrations. The effect of monoRL flushing on the variation in dodecane phase-specific interfacial area is measured by the interfacial partitioning tracer test method.

2. Materials and Methods

2.1. Materials

The monoRL (purity > 98%) used in this study is produced by Zijin Biological Technology Co., Ltd. (Zhejiang, China). *n*-Dodecane (purity \geq 99%), SDBS, and perfluorobenzoic acid (PFBA) were produced by Sigma-Aldrich. All other chemicals were of analytical grade and used as received. All the monoRL solutions were prepared with phosphate-buffer solution (PBS, pH 6.8 ($\text{K}_2\text{HPO}_4 \cdot 3\text{H}_2\text{O}$ 1.35 g/L, KH_2PO_4 1.24 g/L)) as the background solution. The CMC of monoRL in PBS is 157 μM . The hydrophilic glass beads ($d = 0.2\sim 0.4$ mm) were utilized and prepared based on the method described by Zhong et al. [39].

2.2. Experimental Setup and Procedures

The column (2.0 cm in inner diameter, 15.6 cm in length) used in this experiment is made up of glass with connectors made up of stainless steel. It was dry-packed in incremental steps with hydrophilic glass beads and weighed before the column was saturated with water. After the packing process, the column was flushed with carbon dioxide (CO_2) through the column for 10 min to displace air so as to minimize gas entrapment during the subsequent water imbibition phase. It was then saturated with PBS solution, and injected with a rate of 0.29 mL/min into the column in upward flow using a pump. The PBS-saturated column was also weighed and the pore volume (PV) was calculated based on mass balance. Dodecane was then introduced into the column. The dodecane was continuously injected into the column downward until no more water was displaced from the column. To establish a residual saturation of dodecane in the column, PBS was injected at the bottom under flow of 0.29 mL/min and dodecane was displaced from the top end of the column. PBS flooding was ended after no more dodecane displacement in the form of a liquid drop. The residual volume of dodecane in the column was determined gravimetrically.

The IPTT test was conducted to measure the dodecane liquid/water interfacial areas. PFBA (150 mg/L) was used as the nonreactive tracer and low-concentration SDBS (10 mg/L) was chosen as the interfacial partitioning tracer. The PFBA and SDBS were measured sequentially. For tracer tests, a PFBA or SDBS solution was introduced into the column and the solution was collected at the outlet.

The investigation of the influence of monoRL solution flushing on mobilization and solubilization of residual saturation dodecane was conducted by flushing the column with monoRL solutions. The monoRL flushing experiments were conducted at three surfactant concentrations (50 μM , 150 μM , and 500 μM). In order to measure the possible mobilization of dodecane fluid caused by the interfacial tension reduction because of the introduction of monoRL, the column was flushed with surfactant solution firstly for 3 PV for each flushing experiment under a certain monoRL concentration. After the 3 PV monoRL solution flushing, the column was flushed by PBS for at least 12 h and weighed. A new residual saturation is acquired after the first 3 PV monoRL flushing. Then, the ability of monoRL to enhance the solubilization of residual dodecane at the very concentration is measured through the subsequent flushing experiment. The monoRL solution was used to flush the column for about 7 PV and then flush the column with PBS. Samples of effluent were collected with glass tubes. These samples were weighed and measured for concentrations of dodecane and monoRL. In addition, the zeta potential and dynamic light scattering (DLS) size of particles of samples collected at 4~8 PV were measured.

2.3. Analytical Methods

The PFBA concentration of collected effluent at the column outlet was measured using a UV-spectrophotometer at wavelength 260 nm. The SDBS concentration of collected

effluent at the column outlet during column experiments was measured using a UV-spectrophotometer at wavelength 260 nm.

Dodecane concentration is determined using gas chromatography (Agilent 7890A). The measurement method of effluent dodecane concentration is as follows: A pipette was used to draw 1 mL of effluent and the effluent was transferred into a plastic tube. Then, 10% hydrochloric acid (0.05 mL), ethanol (2 mL), and *n*-hexane (1 mL) were added into a plastic tube sequentially. The mixture was vortexed for five minutes and then allowing the mixture to settle for thirty minutes. An amount of 0.75 mL *n*-hexane sample located at the upper phase of the tube was pipetted and measured with gas chromatography (Agilent 7890A) equipped with a flame ionization detector and HP-5 capillary column. The injection volume of the sample is 2 mL with a split injection ratio of 30:1. Temperature of the injection port and detector were 300 °C and 310 °C, respectively. The flow rates of hydrogen, air, and nitrogen are 30, 400, and 20 mL/min, respectively. The exact concentration of dodecane in effluent is calculated by the dodecane concentration standard curve.

JZ-200A (Chengde, China) surface tensiometer with a platinum plate is used to measure the interfacial tension between the organic phase (dodecane) and monoRL solution using the Du Noüy Ring method at 25 °C. The detailed method is as follows: MonoRL solution (15 mL) was pipetted to a 50 mL beaker. Then, dodecane (15 mL) was pipetted and added to the top of the monoRL solution. Before measurement, the beaker was settled for thirty minutes to ensure monoRL partition to the dodecane-water interface. Measurements were reproducible and average results were reported.

The concentration of monoRL was measured with the phenol sulfuric acid method. In brief, 2 mL of the effluent was transferred into a 7 mL centrifuge tube using a pipette. The pH of the sample was adjusted to 2.0 with 1 mol/L hydrochloric acid. Then, 2 mL of ethyl acetate was added and shaken vigorously for 5 min. The upper organic phase was aspirated with a pipette after standing for stratification. The remaining aqueous phase was extracted with ethyl acetate for a total of 3 times. The obtained organic phases were dried at 60 °C. Extracted monoRL was dissolved in a colorimetric tube with 2.0 mL of 0.05 mol/L sodium bicarbonate solution. Then, 1.0 mL of 5% phenol solution and 5.0 mL of concentrated sulfuric acid were added. After 10 min of reaction, the solution was settled for 20 min at 25 °C. The monoRL absorbance was measured at 480 nm using a spectrophotometer.

Measurement methods of Zeta potential and size of monoRL-dodecane aggregates can also be found in Ref. [28]. To evaluate the potential of NAPL mobilization versus trapping of NAPL within a porous medium, one can use dimensionless parameters, such as capillary number (N_C), Bond number (N_B), and trapping number (N_T). Details describing these parameters can be found in previous investigations [40–43].

The SDBS retardation factors were acquired by fitting the BTCs of SDBS with the software of STANMOD. Specific dodecane/water interfacial area (A_{nw} , cm²/cm³) was acquired with the knowledge (Equation (1)) of the interfacial partition coefficient (K_i), equilibrium sorption coefficient (K_s), retardation factor (R), volumetric water content (θ_w), and bulk density (ρ).

$$R = 1 + K_i A_{nw} / \theta_w + K_s \rho / \theta_w \quad (1)$$

The details about the A_{nw} calculation method are described by Saripalli et al. [44].

3. Results and Discussion

3.1. Miscible Displacement of Dodecane

PFBA breakthrough curve (BTC) is shown in Figure 1. The PFBA BTC is sharp and symmetrical for arrival and elution waves, showing uniform ideal transport and uniform packing of the column. Initial monoRL flushing experiments are focused on the displacement of dodecane. Before surfactant flushing, initial dodecane residual saturation is 8.3%. Then, the column is firstly flushed for 10 PV with 10 mg/L SDBS solution so as to avoid the dodecane mobilization caused by SDBS solution flushing. GC measurement results showed no measurable mobilization and solubilization of dodecane occurred. The results of

surfactant flushing experiments indicated that the mobilization of dodecane only occurred in the first 3 PV flushing for each monoRL concentration.

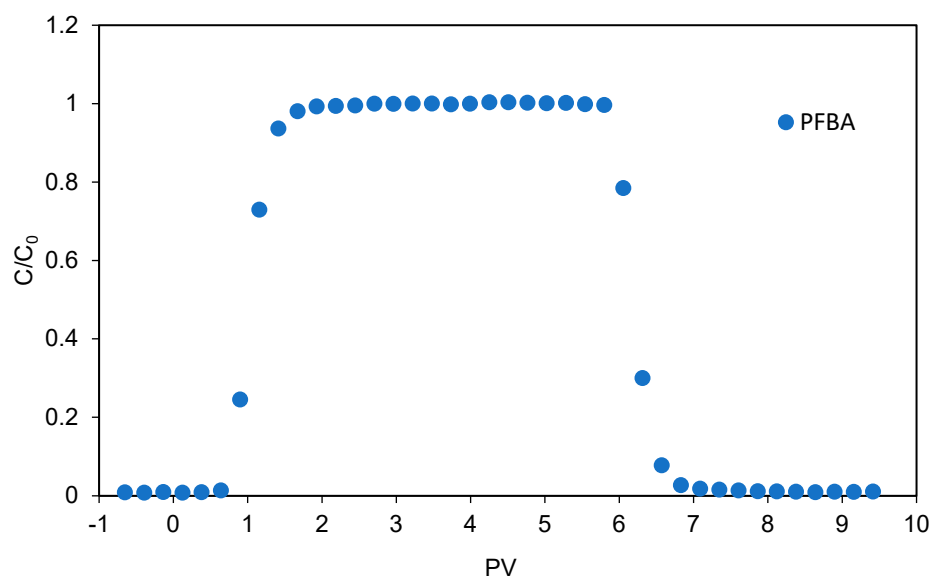


Figure 1. The PFBA-BTC in the PBS saturated column.

The variation in dodecane residual saturation is shown in Table 1. An obvious decrease in dodecane residual saturation occurred when the column was flushed with 50 and 150 μM monoRL solution, while further flushing with a higher concentration (500 μM) of monoRL just caused a tiny decrease in residual saturation. It can be explained by the variation in interfacial tension between the dodecane phase and monoRL solution. In this study, capillary forces are accountable for dodecane trapping because they resist dodecane transport. Capillary forces can be reduced by reducing interfacial tension. Furthermore, buoyancy force may play a role in enhancing the mobilization of dodecane in consideration of the different densities between dodecane and water. The potential of dodecane migration could be evaluated by the parameters of N_C , N_B , and N_T . As shown in Table 1, the value of N_C is close to N_B , which means both N_C and N_B dominate the dodecane displacement procedure. Therefore, it is appropriate to use N_T as the parameter to evaluate the displacement of dodecane caused by monoRL solution flushing. According to a previous study, the magnitude of the trapping number corresponding to the onset of NAPL mobilization is in the order of 10^{-5} [40,41]. With the rise of surfactant flushing solution concentration from 0 to 50, 150, and 500 μM , the interfacial tension between solution monoRL solution and dodecane reduced from 40.7 mN/m to 9.1, 3.3, and 1.1 mN/m. The corresponding N_T increased from 2.62×10^{-5} to 1.18×10^{-4} , 3.25×10^{-4} , and 9.76×10^{-4} , respectively. At the same time, the residual saturation of dodecane decreased from 8.3% to 5.7%, 2.0%, and 1.8%, respectively. Based on the calculation, 78% of dodecane in the column was displaced from the column because of the mobilization caused by the reduction in interfacial tension. We need to note that 76% of dodecane has been displaced out of the column under the flushing of 3PV 150 μM monoRL solution and the change in dodecane saturation is tiny with the monoRL concentration increasing from 150 to 500 μM . It may be attributed to capillary end effects [45]. The effect of surfactant rinsing on the removal of NAPL from a porous medium has been studied by other researchers. For instance, a report from Pennell et al. indicated that the injection of less than 2 pore volumes of a 4% Aerosol AY/OT solution resulted in more than 99% residual PCE recovered from the column [25]. Jaydeep et al. reported that about 37% of NAPL were recovered after the 5 PV flooding of an anionic surfactant [46]. Compared to these studies, monorhamnolipid exhibited an excellent ability to enhance the mobilization of dodecane at lower concentrations. Therefore, monoRL solution flushing at a relatively low concentration may provide an economic method for the remediation

of NAPLs contaminated sites. For instance, at the beginning of remediation, a relatively low concentration (near CMC) monoRL solution can be used to remove most of the NAPL mass in the media based on the mechanism of mobilization. Then, a high concentration of rhamnolipid should be applied to remove the rest of the NAPL by solubilization. It will be more cost-effective this way for the use of rhamnolipid, an expensive biosurfactant.

Table 1. Parameter of dodecane miscible displacement experiments.

Column	Interfacial Tension (mN/m)	Dodecane RS ^a (%)	R ^b	Anw (cm ² /cm ³)	NC ^c	NB ^d	NT ^e
PBS saturated column			1.656				
column with residual saturation dodecane	40.9 ± 0.10	8.3	2.096	2.04	1.08 × 10 ⁻⁵	1.54 × 10 ⁻⁵	2.62 × 10 ⁻⁵
column is flushed with 50 µM monoRL for 3 PV	9.1 ± 0.06	5.7	2.088	2.13	4.87 × 10 ⁻⁵	6.93 × 10 ⁻⁵	1.18 × 10 ⁻⁴
column is flushed with 150 µM monoRL for 3 PV	3.3 ± 0.06	2.0	2.206	3.03	1.34 × 10 ⁻⁴	1.91 × 10 ⁻⁴	3.25 × 10 ⁻⁴
column is flushed with 500 µM monoRL for 3 PV	1.1 ± 0.10	1.8	2.293	3.54	4.03 × 10 ⁻⁴	5.73 × 10 ⁻⁴	9.76 × 10 ⁻⁴

^a Residual saturation; ^b retardation factor; ^c capillary number; ^d Bond number; ^e trapping number.

3.2. Residual Dodecane (NAPL) Solubilization

For each experiment, a 1-D flow solubilization experiment is conducted after the dodecane displacement experiment. Dodecane elution curves acquired from column solubilization experiments are presented in Figure 2. It is obvious that the solubilized dodecane concentration is enhanced at both sub-CMC monoRL concentrations (50 and 150 µM) and above CMC concentration (500 µM). Corresponding solubilized dodecane concentration in the column flushing experiment is 11.4, 14.2, and 158.5 µM, respectively. The solubilized dodecane concentration at sub-CMC concentration is significantly lower than that at hyper-CMC concentration. It indicates a higher concentration of monoRL can result in more remarkable dodecane solubilization, which may be attributed to the presence of enormous quantities of monoRL micelles. The breakthrough curve plateau of dodecane concentration in column experiments is far lower than equilibrium solubilization concentrations in our previous batch solubilization study in which solubility of dodecane in PBS reached 300 and 1100 µM under the concentration of monoRL 50 and 150 µM, respectively [28]. The significant difference may be attributed to lower (0.88 h versus 72 h) contact time in the column experiment than the batch solubilization experiment, monoRL-dodecane aggregate's retention in the porous medium, and dilution effects. Based on our calculation, the recovery of equivalent amounts of 10% of initial residual dodecane in the column by 500 µM monoRL solution flushing solubilization would require about 350 PV of monoRL solution. Therefore, compared to solubilization, displacing dodecane from the column caused by reducing interfacial tension is more economical and effective than surfactant solubilization.

Measurable retardation is observed for monoRL. Compared to the PFBA BTC, there is a stable plateau at a value less than $C/C_0 = 1$ (Figure 3). It indicates that the retention process affected the transport of monoRL, which is irreversible. The results are different from our previous study in which monoRL did not show a retention process during transport in a saturated sandy porous medium containing no NAPL [47]. Based on the observation of DLS measurement results and our previous study [48], monoRL irreversible-retention behavior is due to the existence of monoRL-dodecane aggregates. Figure 4 shows the aggregate size and zeta potential of monoRL-dodecane aggregates in the outlet at BTC plateaus. Aggregate particle size is lower than 550 nm according to DLS measurement data. Therefore, the value of the particle-to-medium size ratio is about 0.003. The ratio is far lower than the empirical threshold (0.05) and it means straining effects will not occur. Therefore, straining is not responsible for the retention [49]. Considering the glass bead is geochemically homogeneous, the mechanism most likely contributing to aggregate retention is sorption on the porous medium surface and at physical heterogeneities. Figure 4

shows that the size of monoRL-dodecane aggregate decreases with the rise in monoRL concentration. It can be explained by the structure of dodecane-monoRL aggregate in our previous investigation. Dodecane-monoRL aggregate was viewed as sphere aggregate with monoRL molecules partitioned at the surface with alkane in the core of the aggregate. The molecules of monoRL approach each other on the surface of the aggregate; with the increase in monoRL concentration, repulsion force between polar groups induces an unequal rate of approach for polar and hydrophobic moieties between molecules, which may cause an increase in aggregate surface curvature and decrease in monoRL-dodecane particle size [50].

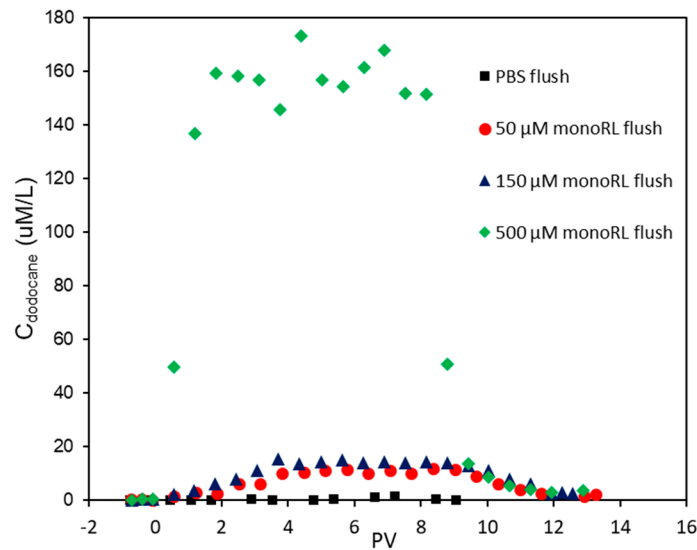


Figure 2. The concentration of dodecane in effluent in 1-D column solubilization tests.

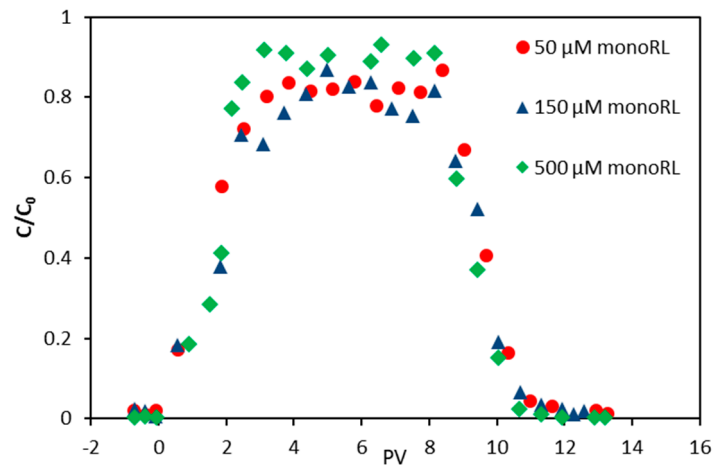


Figure 3. The BTC of monoRL in column solubilization test.

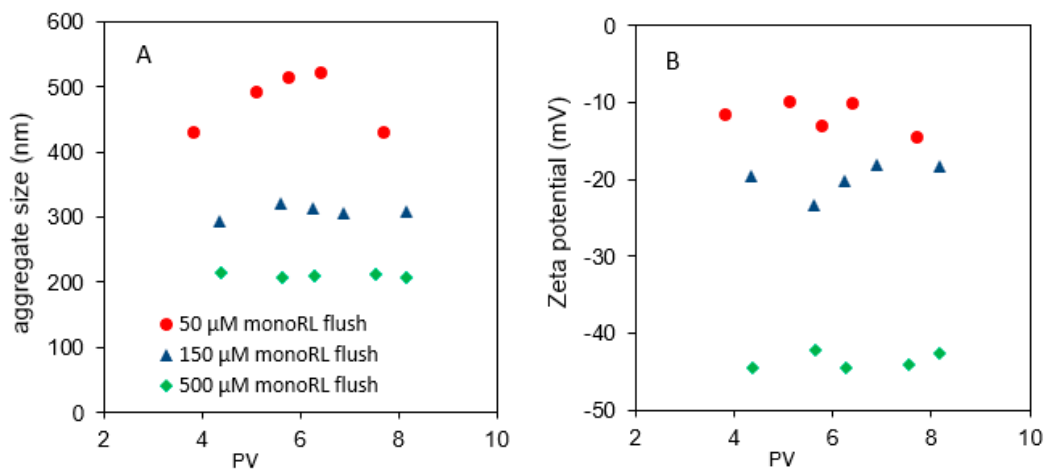


Figure 4. The aggregate size (A) and zeta potential (B) of formed dodecane-monoRL aggregate.

3.3. Interfacial Partitioning Tracer Tests

The results of SDBS tracer tests are shown in Figure 5. The dodecane residual saturation and retardation factors of SDBS obtained by data fitting (Figure 6) with the software of STANMOD and A_{nw} are presented in Table 1. The results show that the flushing of monoRL solution results in an obvious increase in specific dodecane-water interfacial areas. According to experiment data, the decrease in residual saturation of dodecane is significant under the flushing of monoRL solution (Table 1). The increase in specific NAPL-water interfacial areas is likely a result of the occurrence of more tiny dodecane drops and the redistribution of dodecane in the column. For example, Ghosh et al. reported that oil blobs were broken down into smaller blobs and redistributed in a pore-scale study [46]. The increase of A_{nw} is slight under the flushing of 50 μM monoRL solution, while the increase of A_{nw} is significant under the flushing of 150 μM and 500 μM monoRL solution. It may be caused by the more significant interfacial tension decrease for 150 μM and 500 μM monoRL solution flushing than that caused by the 50 μM monoRL solution. The further decrease in interfacial tension may be in favor of the formation of smaller dodecane drops and redistribution. The dodecane-water interface is a crucial variable affecting the dissolution rate [37,51]. For example, Li et al. reported that the oxidation rates of NAPL decreased with the decrease in NAPL-water interfacial areas, on account of the control of NAPL mass transfer into the aqueous phase [52]. Therefore, the ability of monoRL to enhance the NAPL-water interface area may be beneficial to subsequent bioremediation or in-site chemical remediation.

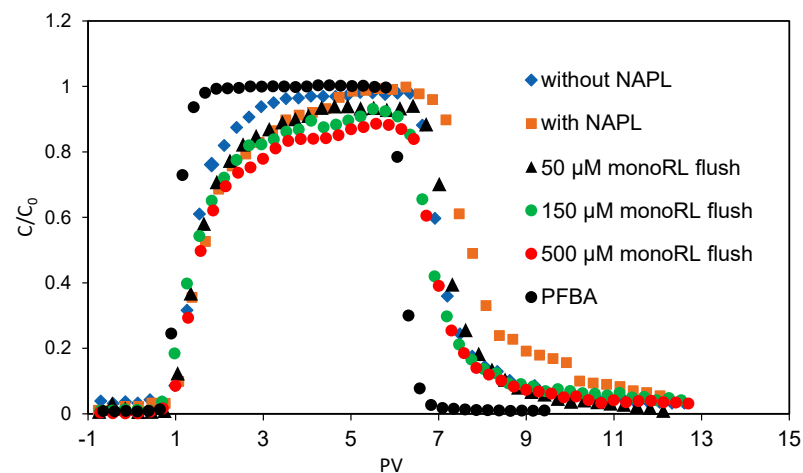


Figure 5. The BTC of SDBS in column experiment.

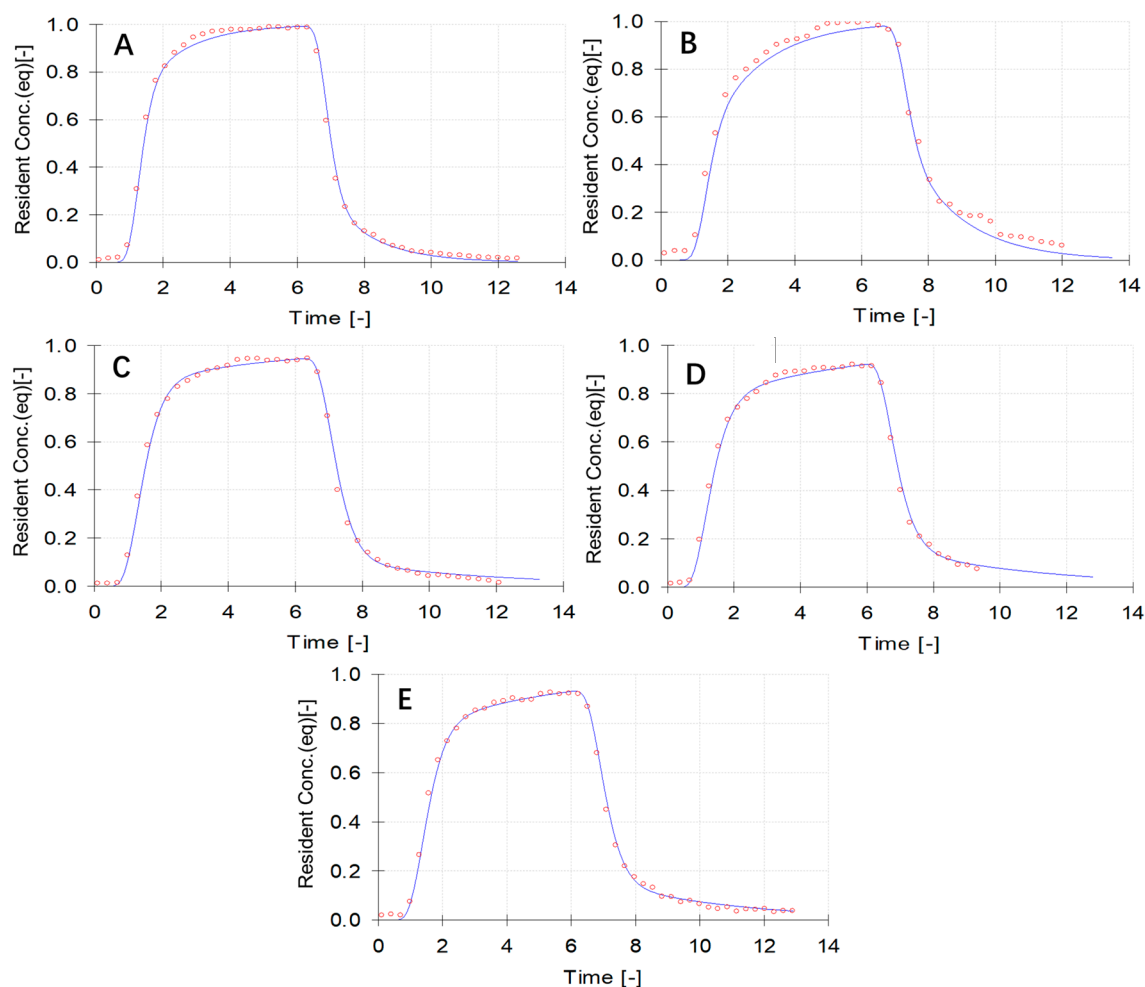


Figure 6. Fitting of SDBS-BTC with two-site chemical nonequilibrium model by STANMOD software. ((A)—PBS saturated column, (B)—column with residual saturation (8.3%) dodecane, (C)—column is flushed with 50 μM monoRL for 3 PV, (D)—column is flushed with 150 μM monoRL for 3 PV, (E)—column is flushed with 500 μM monoRL for 3 PV).

4. Conclusions

Remediating the NAPLs contaminated aquifer is an important issue. Surfactant-enhanced aquifer remediation is a promising technology. This investigation mainly focused on the affecting of monoRL flushing on the mobilization and solubilization of residual dodecane in porous medium. The results of this investigation show that monorhamnolipid biosurfactant is effective in enhancing the removal of residual dodecane in saturated glass bead columns at relatively low concentrations. Miscible displacement is the predominant mechanism for the removal of dodecane. At the same time, this investigation demonstrated solubilization of dodecane in a porous medium can be achieved even at low concentrations and the solubilization is based on the aggregate-formation mechanism. At the solubilization stage, a higher concentration of surfactant should be used. This study implies using a surfactant solution with a significantly higher CMC concentration may be unnecessary at the initial stage, which is helpful for the application of surfactant in remediating NAPL-contaminated sites. These results indicate the potential of monorhamnolipid to apply in the field of surfactant-enhanced aqueous remediation. However, the performance of monoRL in practical applications is influenced by other factors. For example, solution pH, coexisting ions, and soil sorption may influence the performance of monoRL in practical applications. Therefore, field tests on the application of monoRL for remediation should be conducted in the future.

Author Contributions: Conceptualization, H.Z. and X.Y.; methodology, H.Z. and X.Y.; software, G.L. and X.Y.; validation, L.H. and Z.W.; formal analysis, Z.W.; investigation, X.Y.; data curation, X.Y. and L.H.; writing—original draft preparation, X.Y.; writing—review and editing, H.Z. and G.L.; supervision, H.Z. and L.H.; project administration, H.Z. and G.L.; funding acquisition, H.Z. All authors have read and agreed to the published version of the manuscript.

Funding: This study was funded by the National Natural Science Foundation of China (No. 52200200), the Major Science and Technology Projects of Henan Province (221100320200), the Fundamental Research Funds for the Central Universities (2042023kf0163), the Natural Science Foundation of Hubei province (2023AFB228), Yongjiang Talent Introduction Programme of Ningbo (2023A-385-C) and Startup Foundation of Scientific Research of Nanyang Normal University (2024ZX016).

Data Availability Statement: The data that support the findings of this study are available from the corresponding author upon reasonable request.

Conflicts of Interest: The authors declare no conflicts of interest.

References

1. Sharma, P.; Kostarelos, K.; Lenschow, S.; Christensen, A.; de Blanc, P.C. Surfactant flooding makes a comeback: Results of a full-scale, field implementation to recover mobilized NAPL. *J. Contam. Hydrol.* **2020**, *230*, 103602. [[CrossRef](#)] [[PubMed](#)]
2. Mo, Y.Y.; Dong, J.; Zhao, H.F. Field demonstration of in-situ microemulsion flushing for enhanced remediation of multiple chlorinated solvents contaminated aquifer. *J. Hazard. Mater.* **2024**, *463*, 132772. [[CrossRef](#)]
3. Trellu, C.; Mousset, E.; Pechaud, Y.; Huguenot, D.; van Hullebusch, E.D.; Esposito, G.; Oturan, M.A. Removal of hydrophobic organic pollutants from soil washing/flushing solutions: A critical review. *J. Hazard. Mater.* **2016**, *306*, 149–174. [[CrossRef](#)]
4. Fedrizzi, F.; Ramos, D.T.; Lazzarin, H.S.C.; Fernandes, M.; Larose, C.; Vogel, T.M.; Corseuil, H.X. A Modified Approach for in Situ Chemical Oxidation Coupled to Biodegradation Enhances Light Nonaqueous Phase Liquid Source Zone Remediation. *Environ. Sci. Technol.* **2017**, *51*, 463–472. [[CrossRef](#)]
5. Li, Y.; Liao, X.; Huling, S.G.; Xue, T.; Liu, Q.; Cao, H.; Lin, Q. The combined effects of surfactant solubilization and chemical oxidation on the removal of polycyclic aromatic hydrocarbon from soil. *Sci. Total Environ.* **2019**, *647*, 1106–1112. [[CrossRef](#)]
6. Yun, G.; Park, S.; Kim, Y.; Han, K. Development of Slow-Releasing Tablets Combined with Persulfate and Ferrous Iron for In Situ Chemical Oxidation in Trichloroethylene-Contaminated Aquifers. *Water* **2023**, *15*, 4103. [[CrossRef](#)]
7. Hiester, U.; Bieber, L. Dominating Processes of the In Situ Thermal Remediation (ISTR) of low permeable soils. *Grundwasser* **2017**, *22*, 185–195. [[CrossRef](#)]
8. Stroo, H.F.; Leeson, A.; Marqusee, J.A.; Johnson, P.C.; Ward, C.H.; Kavanaugh, M.C.; Sale, T.C.; Newell, C.J.; Pennell, K.D.; Lebron, C.A.; et al. Chlorinated Ethene Source Remediation: Lessons Learned. *Environ. Sci. Technol.* **2012**, *46*, 6438–6447. [[CrossRef](#)]
9. Ramdass, A.C.; Rampersad, S.N. Naturally-occurring microbial consortia for the potential bioremediation of hydrocarbon-polluted sites in Trinidad. *Bioremediat. J.* **2023**, *27*, 443–452. [[CrossRef](#)]
10. Martel, R.; Lefebvre, R.; Gelinat, P.J. Aquifer washing by micellar solutions: 2. DNAPL recovery mechanisms for an optimized alcohol-surfactant-solvent solution. *J. Contam. Hydrol.* **1998**, *30*, 1–31. [[CrossRef](#)]
11. Schwillé, F. *Migration of Organic Fluids Immiscible with Water in the Unsaturated Zone*; Springer: Berlin/Heidelberg, Germany, 1984; pp. 27–48.
12. Mineo, S. Groundwater and soil contamination by LNAPL: State of the art and future challenges. *Sci. Total Environ.* **2023**, *874*, 162394. [[CrossRef](#)] [[PubMed](#)]
13. Javanbakht, G.; Goual, L. Impact of Surfactant Structure on NAPL Mobilization and Solubilization in Porous Media. *Ind. Eng. Chem. Res.* **2016**, *55*, 11736–11746. [[CrossRef](#)]
14. Wu, L.; Zhang, J.; Chen, F.; Li, J.; Wang, W.; Li, S.; Hu, L. Mechanisms, Applications, and Risk Analysis of Surfactant-Enhanced Remediation of Hydrophobic Organic Contaminated Soil. *Water* **2024**, *16*, 2093. [[CrossRef](#)]
15. Liang, X.; Dong, J.; Zhang, W.; Mo, Y.; Li, Y.; Bai, J. Solubilization mechanism and mass-transfer model of anionic-nonionic gemini surfactants for chlorinated hydrocarbons. *Sep. Purif. Technol.* **2024**, *330*, 125534. [[CrossRef](#)]
16. Wang, Z.; Yang, Z.; Chen, Y.-F. Pore-scale investigation of surfactant-enhanced DNAPL mobilization and solubilization. *Chemosphere* **2023**, *341*, 140071. [[CrossRef](#)]
17. Pennell, K.D.; Abriola, L.M.; Weber, W.J. Surfactant-Enhanced Solubilization of Residual Dodecane in Soil Columns.1. Experimental Investigation. *Environ. Sci. Technol.* **1993**, *27*, 2332–2340. [[CrossRef](#)]
18. Taylor, T.P.; Pennell, K.D.; Abriola, L.M.; Dane, J.H. Surfactant enhanced recovery of tetrachloroethylene from a porous medium containing low permeability lenses—1. Experimental studies. *J. Contam. Hydrol.* **2001**, *48*, 325–350. [[CrossRef](#)] [[PubMed](#)]
19. Zhang, M.; Chen, W.; Chuan, X.; Guo, X.; Shen, X.; Zhang, H.; Wu, F.; Hu, J.; Wu, Z.; Wang, X. Remediation of heavily PAHs-contaminated soil with high mineral content from a coking plant using surfactant-enhanced soil washing. *Sci. Total Environ.* **2024**, *909*, 168499. [[CrossRef](#)]

20. Yao, Y.; Fu, Y.; Zhang, C.; Zhang, H.; Qin, C. The effectivity and applicability of a novel sugar-based anionic and nonionic Gemini surfactant synthesized for the perchloroethylene-contaminated groundwater remediation. *J. Hazard. Mater.* **2024**, *478*, 135458. [[CrossRef](#)]
21. Liu, G.; Zhong, H.; Yang, X.; Liu, Y.; Shao, B.; Liu, Z. Advances in applications of rhamnolipids biosurfactant in environmental remediation: A review. *Biotechnol. Bioeng.* **2018**, *115*, 796–814. [[CrossRef](#)]
22. Di Trapani, D.; De Marines, F.; Lucchina, P.G.; Viviani, G. Surfactant-enhanced mobilization of hydrocarbons from soil: Comparison between anionic and nonionic surfactants in terms of remediation efficiency and residual phytotoxicity. *Process Saf. Environ. Prot.* **2023**, *180*, 1–9. [[CrossRef](#)]
23. Wu, M.; Cheng, Z.; Qin, G.X.; Lei, M.; Wu, J.F.; Wu, J.C.; Hu, B.X.; Lin, J. The change of representative elementary volume of DNAPL influenced by surface active agents during long-term remediation period in heterogeneous porous media. *Sci. Total Environ.* **2018**, *625*, 1175–1190. [[CrossRef](#)]
24. Jacome, L.A.P.; Van Geel, P.J. Comparative study of the impacts of soil wettability during entrapped LNAPL removal by surfactant flooding in two different sand media. *J. Soils Sediments* **2015**, *15*, 24–31. [[CrossRef](#)]
25. Pennell, K.D.; Jin, M.Q.; Abriola, L.M.; Pope, G.A. Surfactant enhanced remediation of soil columns contaminated by residual tetrachloroethylene. *J. Contam. Hydrol.* **1994**, *16*, 35–53. [[CrossRef](#)]
26. Ramsburg, C.A.; Pennell, K.D.; Abriola, L.M.; Daniels, G.; Drummond, C.D.; Gamache, M.; Hsu, H.L.; Petrovskis, E.A.; Rathfelder, K.M.; Ryder, J.L.; et al. Pilot-scale demonstration of surfactant-enhanced PCE solubilization at the Bachman Road site. 2. System operation and evaluation. *Environ. Sci. Technol.* **2005**, *39*, 1791–1801. [[CrossRef](#)]
27. Gardner, K.H.; Arias, M.S. Clay swelling and formation permeability reductions induced by a nonionic surfactant. *Environ. Sci. Technol.* **2000**, *34*, 160–166. [[CrossRef](#)]
28. Zhong, H.; Yang, X.; Tan, F.; Brusseau, M.L.; Yang, L.; Liu, Z.; Zeng, G.; Yuan, X. Aggregate-based sub-CMC solubilization of n-alkanes by monorhamnolipid biosurfactant. *New J. Chem.* **2016**, *40*, 2028–2035. [[CrossRef](#)] [[PubMed](#)]
29. Bai, G.Y.; Brusseau, M.L.; Miller, R.M. Biosurfactant-enhanced removal of residual hydrocarbon from soil. *J. Contam. Hydrol.* **1997**, *25*, 157–170. [[CrossRef](#)]
30. Berkowitz, B.; Hansen, D.P. A numerical study of the distribution of water in partially saturated porous rock. *Transp. Porous Media* **2001**, *45*, 303–319. [[CrossRef](#)]
31. Brusseau, M.L.; Popovicova, J.; Silva, J.A.K. Characterizing gas-water interfacial and bulk water partitioning for gas phase transport of organic contaminants in unsaturated porous media. *Environ. Sci. Technol.* **1997**, *31*, 1645–1649. [[CrossRef](#)]
32. Brusseau, M.L.; Narter, M.; Schnaar, S.; Marble, J. Measurement and Estimation of Organic-Liquid/Water Interfacial Areas for Several Natural Porous Media. *Environ. Sci. Technol.* **2009**, *43*, 3619–3625. [[CrossRef](#)] [[PubMed](#)]
33. Saripalli, K.P.; Kim, H.; Rao, P.S.C.; Annable, M.D. Measurement of specific fluid—Fluid interfacial areas of immiscible fluids in porous media. *Environ. Sci. Technol.* **1997**, *31*, 932–936. [[CrossRef](#)]
34. Kim, H.; Rao, P.S.C.; Annable, M.D. Consistency of the interfacial tracer technique: Experimental evaluation. *J. Contam. Hydrol.* **1999**, *40*, 79–94. [[CrossRef](#)]
35. Noordman, W.H.; De Boer, G.J.; Wietzes, P.; Volkering, F.; Janssen, D.B. Assessment of the use of partitioning and interfacial tracers to determine the content and mass removal rates of nonaqueous phase liquids. *Environ. Sci. Technol.* **2000**, *34*, 4301–4306. [[CrossRef](#)]
36. Brusseau, M.L.; Narter, M.; Janousek, H. Interfacial Partitioning Tracer Test Measurements of Organic-Liquid/Water Interfacial Areas: Application to Soils and the Influence of Surface Roughness. *Environ. Sci. Technol.* **2010**, *44*, 7596–7600. [[CrossRef](#)]
37. Dobson, R.; Schroth, M.H.; Oostrom, M.; Zeyer, J. Determination of NAPL-water interfacial areas in well-characterized porous media. *Environ. Sci. Technol.* **2006**, *40*, 815–822. [[CrossRef](#)]
38. Brusseau, M.L.; Taghap, H. NAPL-water interfacial area as a function of fluid saturation measured with the interfacial partitioning tracer test method. *Chemosphere* **2020**, *260*, 127562. [[CrossRef](#)]
39. Zhong, H.; Jiang, Y.; Zeng, G.; Liu, Z.; Liu, L.; Liu, Y.; Yang, X.; Lai, M.; He, Y. Effect of low-concentration rhamnolipid on adsorption of *Pseudomonas aeruginosa* ATCC 9027 on hydrophilic and hydrophobic surfaces. *J. Hazard. Mater.* **2015**, *285*, 383–388. [[CrossRef](#)] [[PubMed](#)]
40. Pennell, K.D.; Pope, G.A.; Abriola, L.M. Influence of viscous and buoyancy forces on the mobilization of residual tetrachloroethylene during surfactant flushing. *Environ. Sci. Technol.* **1996**, *30*, 1328–1335. [[CrossRef](#)]
41. Sheng, J.J. Preferred calculation formula and buoyancy effect on capillary number. *Asia-Pac. J. Chem. Eng.* **2015**, *10*, 400–410. [[CrossRef](#)]
42. Morrow, N.R.; Songkran, B. Effect of Viscous and Buoyancy Forces on Nonwetting Phase Trapping in Porous Media. In *Surface Phenomena in Enhanced Oil Recovery*; Springer: Boston, MA, USA, 1981.
43. Ghosh, J.; Tick, G.R. A pore scale investigation of crude oil distribution and removal from homogeneous porous media during surfactant-induced remediation. *J. Contam. Hydrol.* **2013**, *155*, 20–30. [[CrossRef](#)] [[PubMed](#)]
44. Saripalli, K.P.; Rao, P.S.C.; Annable, M.D. Determination of specific NAPL-water interfacial areas of residual NAPLs in porous media using the interfacial tracers technique. *J. Contam. Hydrol.* **1998**, *30*, 375–391. [[CrossRef](#)]
45. Chukwudeme, E.A.; Fjelde, I.; Abeyasinghe, K.; Lohne, A. Effect of Interfacial Tension on Water/Oil Relative Permeability on the Basis of History Matching to Coreflood Data. *Spe Reserv. Eval. Eng.* **2014**, *17*, 37–48. [[CrossRef](#)]

46. Ghosh, J.; Tick, G.R.; Akyol, N.H.; Zhang, Y. A pore-scale investigation of heavy crude oil trapping and removal during surfactant-enhanced remediation. *J. Contam. Hydrol.* **2019**, *223*, 103471. [[CrossRef](#)] [[PubMed](#)]
47. Zhong, H.; Liu, G.; Jiang, Y.; Brusseau, M.L.; Liu, Z.; Liu, Y.; Zeng, G. Effect of low-concentration rhamnolipid on transport of *Pseudomonas aeruginosa* ATCC 9027 in an ideal porous medium with hydrophilic or hydrophobic surfaces. *Colloid Surf. B* **2016**, *139*, 244–248. [[CrossRef](#)]
48. Zhong, H.; Zhang, H.; Liu, Z.F.; Yang, X.; Brusseau, M.L.; Zeng, G.M. Sub-CMC solubilization of dodecane by rhamnolipid in saturated porous media. *Sci. Rep.* **2016**, *6*, 33266. [[CrossRef](#)]
49. Torkzaban, S.; Bradford, S.A.; van Genuchten, M.T.; Walker, S.L. Colloid transport in unsaturated porous media: The role of water content and ionic strength on particle straining. *J. Contam. Hydrol.* **2008**, *96*, 113–127. [[CrossRef](#)]
50. Yang, X.; Tan, F.; Zhong, H.; Liu, G.S.; Ahmad, Z.; Liang, Q.H. Sub-CMC solubilization of n-alkanes by rhamnolipid biosurfactant: The Influence of rhamnolipid molecular structure. *Colloid Surface B* **2020**, *192*, 111049. [[CrossRef](#)]
51. Annable, M.D.; Jawitz, J.W.; Rao, P.S.C.; Dai, D.P.; Kim, H.; Wood, A.L. Field evaluation of interfacial and partitioning tracers for characterization of effective NAPL-water contact areas. *Ground Water* **1998**, *36*, 495–502. [[CrossRef](#)]
52. Li, M.; Zhai, Y.; Wan, L. Measurement of NAPL-water interfacial areas and mass transfer rates in two-dimensional flow cell. *Water Sci. Technol.* **2016**, *74*, 2145–2151. [[CrossRef](#)]

Disclaimer/Publisher’s Note: The statements, opinions and data contained in all publications are solely those of the individual author(s) and contributor(s) and not of MDPI and/or the editor(s). MDPI and/or the editor(s) disclaim responsibility for any injury to people or property resulting from any ideas, methods, instructions or products referred to in the content.